Table 4. Habitat differences in species richness within Silwood Park. Mean species richness in six habitats sampled at seven spatial scales from 0.01 to 10,000 m^2.

Habitat	Area (m^2)						
	0.01	0.1	1	10	100	1,000	10,000
Grassland	3.5	5.3	9.3	13.4	20.3	31.7	70.5
Woodland	2.0	2.5	3.8	6.8	10.5	27.1	71.5
Built	3.7	7.2	8.4	12.7	31.1	73.3	123.2
Bracken	1.3	1.6	2.0	2.5	4.4	10.7	n.a.
Heath	1.4	2.0	3.1	5.3	11.5	49.0	65
Fallow	4.4	7.4	10.3	14.3	24.1	40.7	83.7

Table 5. The slopes, z, of the scale-to-scale transitions within each of the habitats in Silwood Park. None of the bracken patches was sufficiently large to calculate a slope for the transition to 10,000 m^2.

Habitat	Area (m^2)					
	0.01–0.1	0.1–1	1–10	10–100	100–1,000	1000–10,000
Grassland	0.196	0.238	0.150	0.207	0.184	0.349
Woodland	0.081	0.173	0.242	0.193	0.437	0.439
Built	0.297	0.054	0.174	0.385	0.406	0.214
Bracken	0.064	0.058	0.094	0.274	0.423	n.a.
Heath	0.171	0.192	0.233	0.349	0.640	0.123
Fallow	0.244	0.141	0.119	0.256	0.225	0.320

intermediate scales (hectare to square kilometer) where whole new habitats are added as sample area is increased. At the largest spatial scales (10's to 1000's km^2), z is relatively small ($0.1 < z < 0.4$), reflecting the low turnover-with-distance that characterizes the British flora (*24*). These results raise important questions about the way that population dynamics creates spatial patterns (*30*), and about the way that spatial patterns (e.g., underlying heterogeneity in substrate) affect population dynamics. They also direct attention to the need to develop a more mechanistic understanding of coexistence at small scales (α diversity) and of distance-dependent turnover in species composition at landscape scales (γ diversity).

References and Notes

1. M. L. Rosenzweig, *Species Diversity in Space and Time* (Cambridge Univ. Press, Cambridge, 1995).
2. S. W. Pacala, in *Plant Ecology*, M. J. Crawley, Ed. (Blackwell Science, Oxford, 1997), pp. 532–555.
3. O. Arrhenius, *J. Ecol.* **9**, 95 (1921).
4. F. W. Preston, *Ecology* **43**, 185 (1962).
5. D. W. Goodall, *Biol. Rev.* **27**, 194 (1952).
6. R. A. Fisher, A. S. Corbet, C. B. Williams, *J. Anim. Ecol.* **12**, 42 (1943).
7. J. B. Plotkin *et al.*, *Proc. Natl. Acad. Sci. U.S.A.* **97**, 10850 (2000).
8. J. G. Skellam, *Biometrika* **39**, 346 (1952).
9. J. B. Plotkin *et al.*, *J. Theor. Biol.* **207**, 81 (2000).
10. E. C. Pielou, *An Introduction to Mathematical Ecology* (Wiley Interscience, New York, 1969).
11. M. W. Palmer, P. S. White, *Am. Nat.* **144**, 717 (1994).
12. J. Harte, S. McCarthy, K. Taylor, A. Kinzig, M. L. Fischer, *Oikos* **86**, 45 (1999).
13. W. E. Kunin, *Science* **281**, 1513 (1998).
14. E. F. Connor, E. D. McCoy, *Am. Nat.* **113**, 791 (1979).
15. R. M. May, in *Ecology and Evolution of Communities*, M. L. Cody, J. M. Diamond, Eds. (Harvard Univ. Press, Cambridge, MA, 1975), pp. 81–120.
16. G. Sugihara, *Am. Nat.* **116**, 770 (1980).
17. P. D. Kilburn, *Ecology* **47**, 831 (1966).
18. B. Hopkins, *J. Ecol.* **43**, 409 (1955).
19. R. Condit *et al.*, *J. Ecol.* **84**, 549 (1996).
20. G. Bell, *Am. Nat.* **155**, 606 (2000).
21. I. Hanski, M. Gyllenberg, *Science* **275**, 397 (1997).
22. J. Harte, A. Kinzig, J. Green, *Science* **284**, 334 (1999).
23. G. Sugihara, *Am. Nat.* **117**, 790 (1981).
24. M. J. Crawley, in *Plant Ecology*, M. J. Crawley, Ed. (Blackwell Science, Oxford, 1997), pp. 595–632.
25. G. C. Druce, *The Flora of Berkshire* (Clarendon, Oxford, 1897).
26. H. J. M. Bowen, *The Flora of Berkshire* (Holywell, Oxford, 1968).
27. C. Stace, *New Flora of the British Isles* (Cambridge Univ. Press, Cambridge, ed. 2, 1997).
28. We compared four statistical models for the Silwood data, using log-linear models corrected for overdispersion: a single slope; two piecewise slopes (using the left and right halves of the data); three piecewise slopes (using three, three, and six scales from small to large); and completely idiosyncratic slopes (10 different slopes). Each model was a significant improvement on the one before; deviance declined from 7583.0 to 5276.9 with 2 slopes, 5176.1 with 3 slopes, and 5143.2 with 10 slopes, as df declined from 1485 to 1483, 1480, then 1475.
29. We established 95% confidence intervals by taking 1000 random subsets of species richness data from each adjacent pair of scales, using a sample size that was half the size of the smallest of the two replicates. We used these smaller random subsets to compute 1000 values of z for each transition in scale. Tables 1 and 2 show the 2.5% and 97.5% percentiles for z.
30. B. M. Bolker, S. W. Pacala, *Am. Nat.* **153**, 575 (1999).
31. J. S. Rodwell, *British Plant Communities*, vols. 1 to 5 (Cambridge Univ. Press, Cambridge, 1991–1997).
32. A. Shmida, *Isr. J. Bot.* **33**, 41 (1984).

33. J.E.H. is supported by a Natural Environment Research Council studentship.

2 October 2000; accepted 20 November 2000

Lack of Replicative Senescence in Cultured Rat Oligodendrocyte Precursor Cells

Dean G. Tang,*† Yasuhito M. Tokumoto, James A. Apperly, Alison C. Lloyd, Martin C. Raff

Most mammalian somatic cells are thought to have a limited proliferative capacity because they permanently stop dividing after a finite number of divisions in culture, a state termed replicative cell senescence. Here we show that most oligodendrocyte precursor cells purified from postnatal rat optic nerve can proliferate indefinitely in serum-free culture if prevented from differentiating; various cell cycle–inhibitory proteins increase, but the cells do not stop dividing. The cells maintain high telomerase activity and p53- and Rb-dependent cell cycle checkpoint responses, and serum or genotoxic drugs induce them to acquire a senescence-like phenotype. Our findings suggest that some normal rodent precursor cells have an unlimited proliferative capacity if cultured in conditions that avoid both differentiation and the activation of checkpoint responses that arrest the cell cycle.

Classical replicative cell senescence in cultured human fibroblasts (*1*) is thought to depend on a cell-division counting mechanism, which is based on a progressive shortening and uncapping (*2*) of telomeres with prolonged proliferation, because it can be avoided by overexpression of the catalytic subunit of telomerase (*3–5*). Although proliferating rodent cells in culture tend to maintain telomerase activity and long telomeres (*3–5*), they also often permanently stop dividing and acquire a senescence-like phenotype. It has been suggested that this telomere-independent arrested state, which can also occur in human cells, may reflect a cell cycle checkpoint response to inappropriate culture conditions, rather than an intrinsic limitation imposed by a cell-division counting mechanism

(*3–5*). In this view, normal rodent cells might be able to proliferate indefinitely under appropriate culture conditions.

A third type of cell cycle arrest occurs during normal animal development, when many precursor cells permanently stop dividing and terminally differentiate. Most oligodendrocyte precursor cells (OPCs) in the developing central nervous system, for example, stop dividing and terminally differentiate into oligodendrocytes that myelinate axons (*6*, *7*), although some OPCs persist into adulthood (*8*, *9*). OPCs purified from embryonic rat optic nerve and cultured in serum-free medium containing platelet-derived growth factor (PDGF) and thyroid hormone (TH) stop dividing and terminally differentiate on a schedule that closely resembles that in vivo (*10*). If TH is omitted from the culture medium, however, most OPCs continue to divide and do not differentiate (*10–12*). We have therefore investigated whether the OPCs in these conditions can proliferate indefinitely.

We purified OPCs from postnatal day 7 (P7) rat optic nerve (*11*). We cultured them in serum-free medium containing PDGF without TH, passaged them when they reached near confluence (*12*), and periodically stained them for senescence-associated β-galactosidase (SA–β-Gal), a putative marker of replicative cell senescence (*13*). In eight out of eight experiments, we were able to culture these cells for more than 6 months (the longest cultures for >20 months), without ever observing a SA–β-Gal$^+$ cell (*14*). Cells cultured for 5, 120, and 480 days all expressed high and comparable levels of telomerase activity (*15*). Moreover, >97% of 480-day cells were diploid when analyzed by flow cytometry after propidium iodide staining (*14*).

To determine whether only a small subpopulation of P7 OPCs can divide indefinitely, we plated 60 or 100 purified P7 OPCs in T-25 culture flasks and counted the number of clones that developed after 20 and 30 days. More than 60% of the cells formed clones, and <20% of the cells in most clones died or differentiated (Table 1). We randomly picked 10 clones after 16 days and replated the cells from each clone in separate flasks; in each case, we could propagate the cells for up to 60 days, which is as long as we followed them, suggesting that most P7 OPCs may be able to proliferate indefinitely.

Cells can escape replicative senescence by acquiring mutations that inactivate p53- and Rb-dependent cell cycle checkpoint responses (*3–5*, *16*). To determine whether such responses were maintained in our long-term OPCs, we tested several stimuli that activate checkpoint responses that lead to either cell cycle arrest or apoptosis, including x-irradiation and treatment with the DNA intercalator adriamycin or the proteosome inhibitor *N*-acetyl-Leu-Leu-Norleu-AL (ALLN) (*17*). All three treatments induced rapid apoptosis in 420-day OPCs (Fig. 1, A and B). To test whether the responses were p53-dependent, we infected the OPCs with a retroviral vector (pBabepuro-p53^{175}) encoding a dominant-negative form of p53 (dn-p53) (*18*). We estimated infection efficiency by using a green fluorescence protein (GFP)–encoding retroviral vector (pBird) (*19*). About 50% of the cells were probably infected with the dn-p53 vector, and apoptosis was decreased by about 50% (Fig. 1, A and B), suggesting that most of the dn-p53–infected cells were resistant to the three agents. Thus, long-term OPCs retain at least some p53-dependent checkpoint responses.

Because p53 transcriptionally activates the cyclin-dependent kinase inhibitor (CKI) p21/Cip1 (p21) (*17*), we used Western blotting to examine whether the three agents increased the level of p21 in long-term (420-day) OPCs. Induction of p21 by these agents was indeed observed, and the increase was partially inhibited in cultures infected with the dn-p53 vector (Fig. 1C), suggesting that the p53 expressed by long-term OPCs is transcriptionally active.

Most normal cells activate a checkpoint response when excessively stimulated to proliferate (*3*, *5*, *21–23*). Overexpression of oncogenic Ras^{V12} (*21*) or Raf (*18*), for example, induces many normal cells to undergo cell cycle arrest, with or without other features of replicative senescence; in contrast, most immortalized cell lines respond by enhanced cell proliferation (*3*, *5*, *16*, *21–23*). When 450-day OPCs were infected with a retroviral vector that coexpressed GFP and Ras^{V12} from separate promoters (pBird-Ras^{V12}) (*19*), the GFP$^+$ cells arrested, as indicated by a decrease in the incorporation of bromodeoxyuridine (BrdU) (Fig. 2, A to C). Overexpression of Ras^{V12} also increased the level of p21 protein (Fig. 1D) and decreased cell proliferation assessed in clonal cultures (Fig. 2, D to F), although it did not result in a senescence-like phenotype (cell flattening or expression of SA–β-Gal activity) (*14*).

Long-term OPCs also displayed contact inhibition of proliferation. When cultured to confluence and assessed by flow cytometry after staining with propidium iodide, for example, about 90% of the cells were in the G_1 phase of the cell cycle, compared with about 60% in subconfluent cultures (*14*). Moreover, the confluent cells predominantly expressed the hypophosphorylated, active form of the Rb protein (Fig. 3A). Because contact inhibition of prolif-

MRC Laboratory for Molecular Cell Biology, University College London, London WC1E 6BT, UK.

*Present address: Department of Carcinogenesis, University of Texas M.D. Anderson Cancer Center, Science Park Research Division, Smithville, TX 78957, USA.

†To whom correspondence should be addressed. E-mail: dtang@sprd1.mdacc.tmc.edu

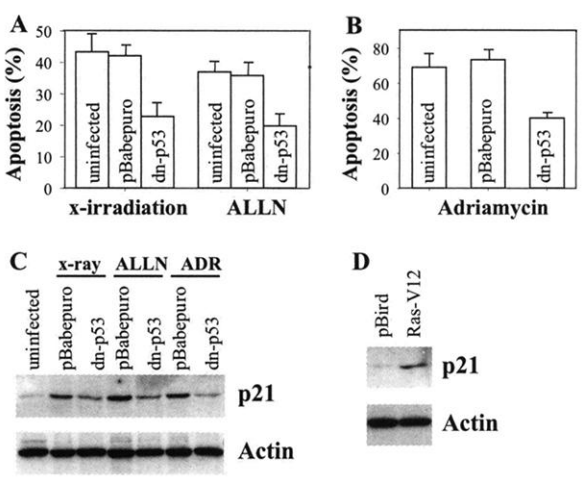

Fig. 1. Apoptosis and p21 induction in OPCs cultured in PDGF without TH for 420 days. (**A** and **B**) Apoptosis induced by x-irradiation or the proteosome inhibitor ALLN (A) or by adriamycin (B). The response was partially inhibited in cultures infected with a retrovirus encoding a dominant-negative p53 (dn-p53). The results are shown as the mean ± SEM of three experiments. The results in (A) were obtained by flow cytometry analysis after propidium iodide staining, whereas those in (B) were obtained by counting pyknotic nuclei after Hoechst dye staining. The inhibition with dn-p53 in all three cases is statistically significant ($P < 0.01$, Student's t test). (**C**) Western blotting showing induction of p21 by x-irradiation (x-ray), ALLN, or adriamycin (ADR) and inhibition by dn-p53. The cells were analyzed 24-hours after treatment. Untreated OPCs that were infected with either the control (pBabepuro) or dn-p53 (pBabepuro-p53^{175}) vector had low levels of p21, similar to the levels in uninfected OPCs (*14*). (**D**) Western blotting showing induction of p21 by oncogenic Ras in OPCs 5 days after infection with pBird or pBird-Ras^{V12} (Ras-V12).

Table 1. Clonal analysis of P7 OPCs. Purified P7 OPCs were plated in a T25 flask and cultured without passaging in PDGF.

Number of cells per flask	Number of clones formed	Number of clones per flask with >80% cells alive
	Day 20	
60	41 (68%)	25 (61%)
100	62 (62%)	42 (73%)
	Day 30	
60	41 (68%)	23 (56%)
100	63 (63%)	49 (78%)

eration is usually Rb-dependent (*24*), these results suggest that the long-term OPCs maintain at least some Rb-dependent checkpoint responses. We also examined whether overexpression of the CKI p16/INK4a (p16) would arrest the cell cycle, because such an arrest usually requires functional Rb (*25*). We infected 330-day OPCs with retroviral vectors encoding either wild-type p16 or a point mutant (p16P48L) that lacks Cdk-binding activity (*26*), both of which were tagged with a hemagglutinin (HA) epitope. Wild-type p16, but not the mutant form, strongly inhibited BrdU incorporation (Fig. 3B). Because the infection efficiency assessed by HA antibody staining was ~30%, it seems likely that most OPCs that overexpressed p16 did not incorporate BrdU.

To determine whether OPCs are capable of acquiring a senescence-like phenotype, we cultured young (5 day) and long-term (510 day) OPCs in 15% fetal bovine serum (FBS), which has been shown to induce OPCs to express glial fibrillary acidic protein (*27*). Within 2 to 3 weeks, both young and long-term OPCs stopped dividing, as assessed by BrdU incorporation; >90% expressed SA–β-Gal activity, and some had a flattened morphology (Fig. 4). When young OPCs were washed after 3 weeks and cultured in serum-free medium containing PDGF and BrdU for another 5 days, no BrdU incorporation was seen, suggesting that the cells may have permanently withdrawn from the cell cycle (*14*). We could also induce OPCs to adopt a senescence-like phenotype by treating them with low doses of genotoxic drugs that induce a senescence-like phenotype in other cell types (*28*). When treated with the DNA polymerase inhibitor aphidicolin (0.25 μg/ml) or adriamycin (5 nM) for 3 days, for example, about 20% of 510-day OPCs became SA–β-Gal$^+$, whereas none did in vehicle-treated cultures (*14*).

Because increases in CKIs, p53, and p19^{ARF} have been implicated in replicative cell senescence (*3–5*, *16*, *21–23*), we analyzed these proteins in proliferating OPCs by Western blotting. All three Cip/Kip family of CKIs—p21, p27, and p57—increased with time in culture (Fig. 5, A and B). Of the four INK4 CKIs—p15, p16, p18, and p19—only p18 and p19 increased, and they then decreased again (Fig. 5A); we could not detect p16 protein at any time (although we could detect it in late-passage rat Schwann cells) (Fig. 5C), and we could detect p16 mRNA only after a second round of reverse transcription–polymerase chain reaction (RT-PCR) amplification, and the level did not change with time in culture (*14*). p53 was barely detectable in OPCs cultured for 10 and 90 days, but it increased greatly by 390 days (Fig. 5A). Because none of the antibodies to p19^{ARF} recognized the rat protein, we used RT-PCR to assess p19^{ARF} mRNA level (*29*) and found that it increased progressively (Fig. 5D). Thus, although the levels of several negative cell cycle regulators increased in OPCs with time in culture, the cells continued to proliferate.

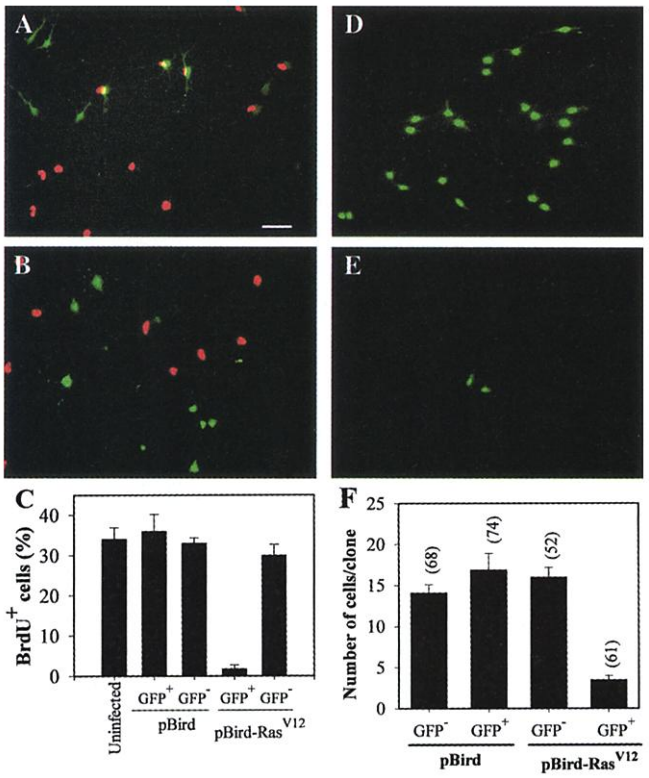

Fig. 2. Oncogenic Ras (Ras^{V12}) induces cell cycle arrest and inhibits clonal expansion in long-term OPCs. (**A** to **C**) BrdU incorporation 5 days after infection of 450-day OPCs. (A and B) Representative fluorescence micrographs showing OPCs infected with pBird (A) or pBird-Ras^{V12} (B) and stained for BrdU after a 4-hour pulse with BrdU (*12*). In (A), many GFP$^+$ cells (green) are also BrdU$^+$ (red), whereas in (B), most GFP$^+$ cells are BrdU$^-$. (C) Mean ± SEM of counts from duplicate flasks for each condition from two separate experiments. More than 1000 cells were counted for each condition. (**D** to **F**) Clonal analyses of 510-day OPCs. (D) and (E) Representative fluorescence micrographs showing typical GFP$^+$ clones 8 days after infection with either pBird (D) or pBird-Ras^{V12} (E). The cells were replated at clonal density 24 hours after infection and cultured for an additional 7 days before counting. (F) Results are shown as the mean ± SEM of counts from duplicate flasks for each condition from two separate experiments. The numbers of clones counted are shown in parentheses. In (C) and (F), the differences between pBird-Ras^{V12}–infected cells and all other conditions are statistically significant ($P < 0.01$, Student's t test). Bar, 10 μm.

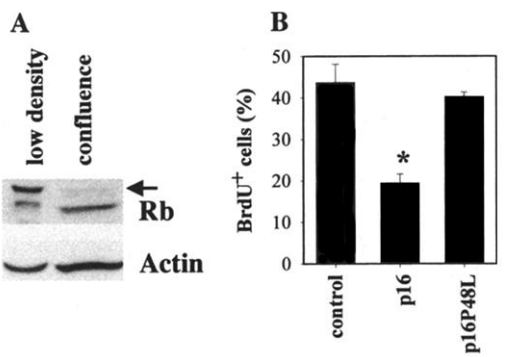

Fig. 3. Rb-dependent checkpoint in long-term OPCs. (**A**) Hypophosphorylation of pRb in confluent cells. The arrow indicates hyperphosphorylated Rb protein. (**B**) Overexpression of wild-type p16 (p16), but not mutant p16 (p16P48L), inhibits BrdU incorporation in 330-day OPCs. Results are shown as the mean ± SD of 1000 to 1500 cells counted for each condition. *$P < 0.01$, Student's t test.

To understand why long-term OPCs continued to proliferate despite the high levels of negative cell cycle regulators, we analyzed various positive cell cycle regulators, including cyclins and Cdks, and compared OPCs to senescent rat fibroblasts. Cdk 2 and 4 and cyclins D1, D3, and E increased in OPCs between 10 days and 390 days (Fig. 5E), perhaps compensating for the increases in the negative cell cycle regulators. Senescent rat fibroblasts expressed lower levels of all of these proteins (Fig. 5E).

Does the unlimited proliferative capacity of OPCs depend on their acquiring immortalizing mutations? Although we cannot exclude this possibility, we think it is unlikely for several reasons. (i) Both young and long-term cultured OPCs express telomerase activity and therefore apparently do not need mutations to maintain their telomeres. (ii) OPCs in our culture conditions do not undergo typical replicative senescence or crisis, with the outgrowth of occasional colonies, as might be expected with mutation and then selection of immortalized cells. (iii) Our clonal analyses suggest that the majority of P7 OPCs have the ability to form clones in culture, most of which can apparently be propagated indefinite-

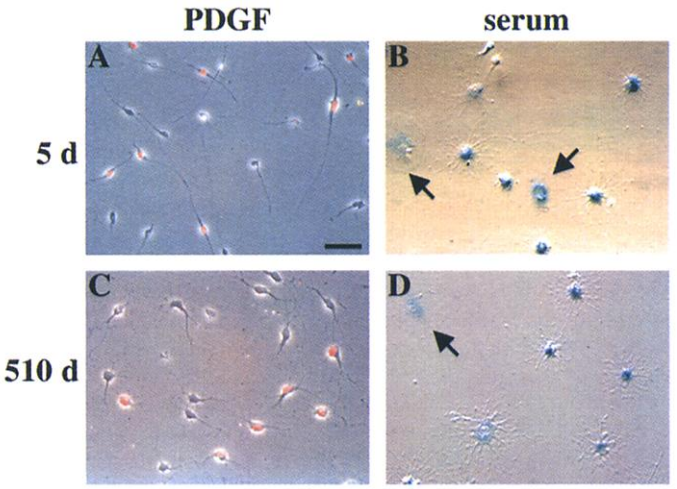

Fig. 4. Serum induces a senescence-like phenotype in OPCs. Five-day (**A** and **B**) or 510-day (**C** and **D**) OPCs were cultured in either serum-free medium containing PDGF [(A) and (C)] or the same medium containing 15% FBS [(B) and (D)] for either 2 weeks [(A) and (B)] or 3 weeks [(C) and (D)]. BrdU was added for the final 4 hours, and the cells were then stained for BrdU incorporation (*12*) and processed for SA–β-Gal activity (*13*). $BrdU^+$ cells are stained red, and SA–$β$-Gal^+ cells are stained blue. Images in (A) and (C) were obtained with phase contrast optics, whereas those in (B) and (D) were obtained with differential interference contrast. Some of the blue cells have a flattened morphology (arrows). All the images are at the same magnification. In serum-free cultures at either age, there were no SA–$β$-Gal^+ cells, and ~40% of the cells were $BrdU^+$; in serum-containing cultures at either age, >90% of the cells were SA–$β$-Gal^+, and, by 3 weeks, none were $BrdU^+$. Bar, 10 μm.

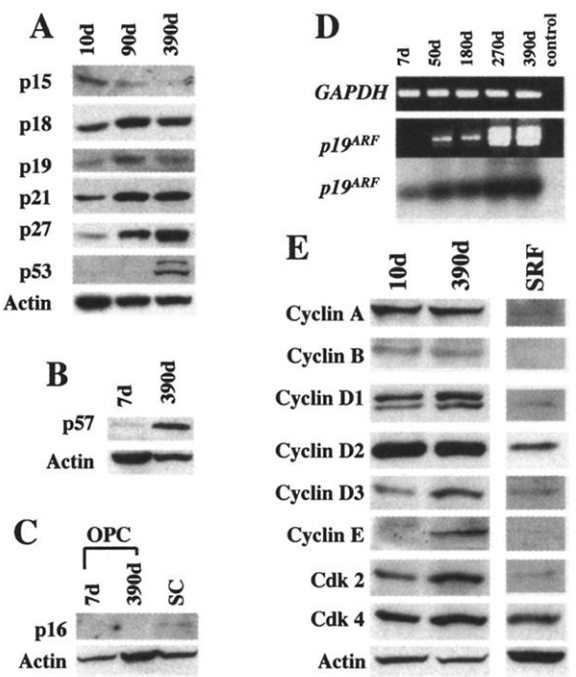

Fig. 5. Changes in cell cycle regulators. (**A**) Western blots of p53 and CKIs in OPCs. The results shown are from two blots that were sequentially probed, stripped, and reprobed for various proteins. (**B**) Western blot of p57 in OPCs. (**C**) Western blot of p16 in OPCs and Schwann cells. SC, rat Schwann cells at passage 22. (**D**) RT-PCR (upper two panels) and Southern blot (lower panel) analysis of $p19^{ARF}$ mRNA levels in OPCs. GAPDH mRNA was analyzed as a positive control (*12*). In the control lane, template RNA was omitted. (**E**) Western blots of cyclins and Cdks. The results are from two blots that were sequentially probed, stripped, and reprobed for the various proteins. We were unable to detect Cdk6 in OPCs at any time in culture (*14*). SRF, senescent rat fibroblasts. For Western blots, 100 μg of total protein was run in each lane, except for Schwann cells in (C) and all lanes in (E), where 60 μg and 50 μg were run, respectively.

ly. (iv) The long-term OPCs maintain Rb- and p53-dependent checkpoint responses, which are often inactivated by mutations that immortalize other rodent cell types (*3*–*5*). (v) The long-term OPCs arrest in response to oncogenic Ras, which generally promotes proliferation of immortalized cells (*21*–*23*). (vi) The long-term OPCs can be induced to undergo rapid cell cycle arrest and to adopt other features of senescence if the culture conditions are altered.

Our findings and those of Mahon *et al.* (*30*) raise the possibility that many types of normal rodent cells may be able to proliferate indefinitely in appropriate culture conditions. They also support the idea that suboptimal culture conditions, or "culture shock," can activate checkpoint responses in both rodent and human cells that lead to permanent cell-cycle arrest and a senescence-like phenotype (*3*, *4*). Human cells without telomerase activity have, in addition, a telomere-based mechanism that will stop proliferation eventually, even under optimal culture conditions (*3*–*5*). It might be best to reserve the phrase "replicative cell senescence" for this telomere-based arrest, as previously suggested (*4*).

References and Notes

1. L. Hayflick, *Exp. Cell Res.* **37**, 614 (1965).
2. E. H. Blackburn, *Nature* **408**, 53 (2000).
3. C. J. Sherr, R. A. DePinho, *Cell* **102**, 407 (2000).
4. W. E. Wright, J. W. Shay, *Nature Med.* **6**, 849 (2000).
5. D. Hanahan, R. A. Weinberg, *Cell* **100**, 57 (2000).
6. B. A. Barres, M. C. Raff, *Neuron* **12**, 935 (1994).
7. M. C. Raff, B. Durand, F.-B. Gao, *Int. J. Dev. Biol.* **42**, 263 (1998).
8. C. ffrench-Constant, M. C. Raff, *Nature* **319**, 499 (1986).
9. G. Wolswijk, M. Noble, *Development* **105**, 387 (1989).
10. F.-B Gao, J. A. Apperly, M. C. Raff, *Dev. Biol.* **197**, 54 (1998).
11. B. A. Barres, M. A. Lazar, M. C. Raff, *Development* **120**, 1097 (1994); see also (*14*) for detailed methods.
12. D. G. Tang, Y. M. Tokumoto, M. C. Raff, *J. Cell Biol.* **148**, 971 (2000).
13. G. P. Dimri *et al.*, *Proc. Natl. Acad. Sci.U.S.A.* **92**, 9363 (1995).
14. D. G. Tang, Y. M. Tokumoto, J. A. Apperly, A. C. Lloyd, M. C. Raff, data not shown.
15. Web Fig. 1 and supplementary material are available on *Science* Online at www.sciencemag.org/cgi/content/full/291/5505/864/DC1.
16. C. J. Sherr, *Genes Dev.* **12**, 2984 (1998).
17. A. J. Giaccia, M. B. Kastan, *Genes Dev.* **12**, 2973 (1998).
18. A. C. Lloyd *et al.*, *Genes Dev.* **11**, 663 (1997).
19. The pBird vector permits the coexpression of GFP and a gene of interest from separate promoters. The SV40-puromycin resistance gene cassette in pBabe-puro retroviral vector (*20*) was replaced with a PCR-amplified cytomegalovirus–enhanced green fluorescence protein (CMV-EGFP) expression cassette from pEGFP-C1 (Clontech). pBird-Ras^{V12} was constructed by subcloning Ras^{V12} sequence into the Bam HI–Eco RI sites of pBird. All retroviral vectors were verified by sequencing. Viruses were harvested from supernatants of transfected Phoenix packaging cells.
20. J. P. Morgenstern, H. Land, *Nucleic Acids Res.* **18**, 3587 (1990).
21. M. Serrano, A. W. Lin, M. E. McCurrach, D. Beach, S. W. Lowe, *Cell* **88**, 593 (1997).
22. C. J. Sherr, J. M. Roberts, *Genes Dev.* **13**, 1501 (1999).
23. A. C. Lloyd, *Curr. Opinion Genet. Dev.* **8**, 43 (1998).
24. N. Dyson, *Genes Dev.* **12**, 2245 (1998).
25. M. Ruas, G. Peters, *Biochim. Biophys. Acta* **1378**, F115 (1998).
26. M. Ruas, S. Brookes, N. Q. McDonald, G. Peters, *Oncogene* **18**, 5423 (1999).
27. M. C. Raff, R. H. Miller, M. Noble, *Nature* **303**, 396 (1993).
28. B. D. Chang *et al.*, *Cancer Res.* **59**, 3761 (1999).
29. Total RNA was isolated and cDNA synthesis carried out with random hexamers. Two microliters of the cDNA was used for PCR. $p19^{ARF}$ mRNA was amplified with primers 5′-GCCACTGCTGGGAGAGTTCGGCC-3′ and 5′-ACCACGTCATGATGGTCTCAC-3′ (93°C for 1 min, 52°C for 1 min, and 72°C for 1 min; 28 cycles). The PCR of glyceraldehyde phosphate dehydrogenase (GAPDH) was carried out as a control (*12*). For Southern blotting, 20-μl PCR products were transferred to a nylon membrane (Hybond-N^+, Amersham) and hybridized with ^{32}P-labeled full-length cDNA of murine $p19^{ARF}$.
30. N. F. Mathon, D. S. Malcolm, M. C. Harrisingh, L. Cheng, A. C. Lloyd, *Science* **291**, 872 (2001); published online (19 January 2001) 10.1126/science.1056782.

31. We thank J. Scholes for help with x-irradiation, S. Brookes and G. Peters for providing pBabepuro-2HA-p16 and pBabepuro-2HA-p16P48L, M. Aldaz for metaphase spread experiments, and A. Mudge and the members of the Raff and Lloyd labs for discussion and support. D.G.T is a recipient of a Hitchings-Elion Award from Burroughs-Wellcome Fund. Y.M.T., J.A.A., and M.C.R are supported by grants from the Medical Research Council, and A.C.L. is supported by the Cancer Research Campaign.

20 October 2000; accepted 3 January 2001
Published online 19 January 2001; 10.1126/science.1056780
Include this information when citing this paper.